High-Energy Compton Scattering

Sahar Khashayar[1, *] and Em Mcglone[1, †]

[1] *Department of Physics, Harvard University, Cambridge, Massachusetts 02138, USA*

(Dated: November 16, 2021)

The Compton shift is the decrease in X-ray or gamma-ray energy resulting that accompanies the scattering of photons off electrons. The reduction of energy and increase in wavelength is related to the angle under Compton's law. In this experiment, we use gamma rays produced by radiation sources $^{137}_{55}$Cs and $^{241}_{95}$Am, and scatter them on copper, aluminum, and carbon scattering targets. The amount of gamma rays received is related to the angle under the Klein-Nishina formula. We compared our findings of the Klein-Nihsina relation against the ideal form of the equation.

I. INTRODUCTION

Wave-particle duality is a quantum mechanical concept that states that every particle can be described as either a particle or a wave. Quantum scale objects cannot be fully adequately described by the classical concepts of "wave" or "particle," but together, they create a complete picture of how particles behave. Wave-particle duality is most notably used to describe the behavior of light. Through the work of several experimentalists and theorists in the early 20th century, such as Albert Einstein, Louis de Broglie, and many more, the wave-particle duality of light and other quantum particles has been verified. One such effect illustrating this duality is known as Compton scattering.

Compton scattering, first observed by Arthur Holly Compton, is the inelastic scattering of a photon off a charged particle, usually an electron. The wavelength of the scattered light is different from the initial wavelength. The amount that the wavelength is shifted is referred to as the Compton shift [1]. The relation for the Compton shift is given by the following equation [2]:

$$\lambda' - \lambda = \frac{h}{m_0 c}(1 - cos\theta) \tag{1}$$

where λ' is the shifted wavelength, λ is the incident wavelength, h is Planck's constant, m_0 is the rest mass of the electron, c is the speed of light, and θ is the scattering angle. A diagram of the scattering from [2] is shown in Figure 1.

This effect is noteworthy because it indicates that light cannot be treated as purely a wave: classical models of electromagnetic scattering have no way of accounting for this shifted wavelength. Compton's experiment shows that, in addition to a wave, light can be treated as a stream of particles, with energies proportional to their wavelength.

This simple theory of Compton scattering is valid for high energy gamma rays. At lower energies, the radiation behaves closer to Thomson scattering, in which the photon frequency and wavelength is not altered by the collision and the charged particle retains its initial energy.

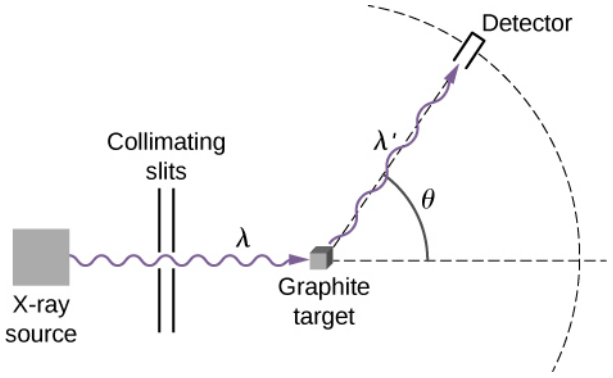

FIG. 1: A diagram showing an incoming X ray being Compton scattered off a graphite target. The relation between λ, λ', and θ is given in Equation 1.

Later, in 1928, O. Klein and Y. Nishina further investigated Compton scattering based on the Dirac equation for the relativistic electron that had been proposed earlier that year. They derived the Klein-Nishina formula for the scattering cross-section of the photon. The form of this equation used in our experiment is expressed in Equation 2:

$$\frac{d\sigma}{d\Omega} = \frac{1}{2} r_e^2 \left(\frac{\lambda}{\lambda'}\right)^2 \left[\frac{\lambda}{\lambda'} + \frac{\lambda'}{\lambda} - \sin^2(\theta)\right] \tag{2}$$

where $\frac{d\sigma}{d\Omega}$ is the differential cross section, $d\Omega$ is an infinitesimal solid angle element, r_e is the classical electron radius ($r_e^2 = 79.406$ milli-barns) in size, and λ, λ', and θ are the incoming and reflected wavelength and the scattering angle, just as in the Compton shift equation 1 [3].

Initially, Compton performed his experiment with X-rays, but eventually expanded his work to include high energy gamma rays [4]. Similarly, we used gamma ray sources in this experiment to verify Compton's findings. We used $^{137}_{55}$ Cs (at 661.7 keV) and $^{241}_{95}$ Am (at 59.6 keV). We measured the Compton shifts for both sources at angles ranging from 10 to 150 degrees, with scattering targets of graphite, aluminum, and copper. We also created our own graph of the photon cross-sectional area

* skhashayar@college.harvard.edu
† mdmcglone@college.harvard.edu

and compared this to the ideal form of the Klein-Nishina formula.

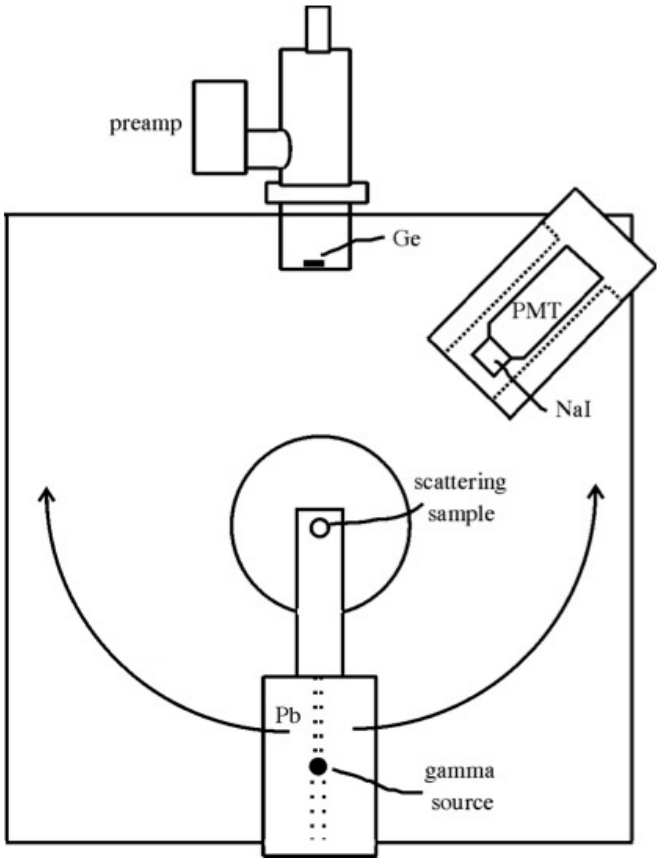

FIG. 2: A diagram of the Compton scattering apparatus. The germanium detector is at the top, connected to a preamp as part of the setup for the gamma ray spectrometer. The sodium iodide scintillation detector is at the top right. The scattering sample is mounted on the bottom; it can be rotated with an angle relative to either detector. The scattering target is mounted in the center.

II. SETUP/APPARATUS

A diagram of the apparatus is shown in Figure 2. It includes the gamma ray sources (the cesium or the americium), a sodium iodide scintillation detector and a germanium detector, and the gamma ray spectrometer, which includes a high voltage power supply, preamp, spectroscopy amp, multi-channel analyzer.

Since the Cesium and Americium sources emit gamma rays of different energies, we used two different detectors, the sodium iodide scintillation detector, which is more efficient at high energies, and the germanium detector for the lower energies. At lower energies, the Compton shift is relatively small, and so we use the higher resolution germanium detector. The germanium detector's efficiency decreases drastically at higher energies (from 100% efficiency at 60keV down to .02% efficiency at 1MeV), so for higher energies we use the scintillation detector.

A. Gamma Ray Sources and Scattering Targets

The source shield and beam collimator is a 5" diameter x 8" long lead cylinder (in a copper casing), which is able to be rotated around relative to the two detectors. A hole runs down its central axis. The gamma source is inserted all the way in the 1/2" diameter entrance hole, and the 1/4" diameter exit hole collimates the beam. We had several different scattering targets available for use, in both plate and cylinder form. The targets are held by a 3/16" diameter post at the center of rotation of the source. 25lb lead bricks can be used to shield areas from the radioactive source. The scattering angle itself can be varied by rotating the source around the scatterer.

B. Scintillation Detector

The detector is a cylindrical thallium doped sodium iodide scintillation crystal coupled to a photomultiplier tube (PMT), sealed in an aluminum container. When gamma rays enter the scintillation crystal, they lose energy in the crystals via Compton scattering and the photoelectric process. The resulting energized electrons ionize the thallium phosphor, and decay by emitting visible light that is then detected by the PMT. The detector is shielded from background radiation by a lead cylinder (1" thickness) and magnetically by a mu-metal shield.

C. Ge Detector

The germanium detector consists of semiconductor diodes with a PIN diode structure, in which the intrinsic (I) region is sensitive to ionizing radiation. When photons interact with the material in the intrinsic region, electrons and positive electron-holes are produced and are swept by the electric field to the P and N electrodes. This charge pulse is converted into a voltage pulse by a capacitor and integral preamplifier.

Because germanium has a relatively small band gap, the detector must be cooled in order to reduce the leakage current to an acceptable level. Otherwise, leakage current induces noise that would ruin the resolution of the detector. The detector is mounted in a vacuum chamber, which is inserted into a 30 liter liquid nitrogen tank, protecting its sensitive parts.

D. Multi-Channel Analyzer (MCA)

The detector output consists of pulses of variable amplitude, with amplitude proportional to the energy of the radiation. The pulse height distribution is stored by the

pulse height analyzer (PHA; Ortec 926 ADCAM MCB, a NIM module with USB interface), which plots the number of pulses as a function of the peak voltage (which relates to the gamma ray energy).

The software that controls the PHA is called MAESTRO. This software gives a histogram of the pulse heights, thereby recording the frequency of gamma rays at different energies reaching the detector.

III. EXPERIMENT

Through the experiment, we worked first with the high-energy Compton shifts with the sodium iodide detector with a cesium source, and then moved onto the low-energy Compton shifts with an americium source. For both detectors, we first used calibration cesium and americium sources to calibrate the detector and the data collection software. Smaller sources were placed in front of the detectors, and we adjusted the gain and voltage on the MCA to place the 661.7 keV cesium peak and the 59.6 keV americium peak near the top of the software's range. From there, we recorded the positions of the calibration peak and used that as a reference point to compare the shifted peaks to.

Once the detectors were calibrated, we moved on to using the proper Cs-137 and Am-241 sources. For each source, we picked a scattering target and measured the Compton shift around several angles.

In order to properly determine the Klein-Nishina relations for the sources, we needed to find the solid angle between the scattering target and the detector. We first found the active area of the detectors by placing lead bricks on either side of the detector, and decreasing the distance between them until they blocked off the radiation from the detector. The point at which the radiation started to be blocked is the actual active area for the detector, which for the sodium iodide detector was at 3cm (pretty much the full detector area), and for the germanium detector was at 1.5cm.

We then used the following equation to calculate the solid angle for the detector:

$$\text{solid angle} = \frac{\pi r^2_{\text{detector}}}{4\pi r^2_{\text{scattering}}} \tag{3}$$

The solid angle we obtained for the sodium iodide detector was .00287 square radian. For the germanium detector, it was .000717 square radian.

A. High Energy Compton shifts

We measured the Compton shifts from the cesium gamma rays at various angles (10, 30, 60, 90, 120, and 150 degrees, as shown in figure XYZ – table) using copper as a scattering target. This scattering target is a 3" copper cylinder with a 1/2" diameter. The proper wavelength for the Cs-137 gamma ray with energy 661.7 kev is 1.87 pm, and so all of our ideal Compton shift wavelengths are derived from this wavelength using Equation 1.

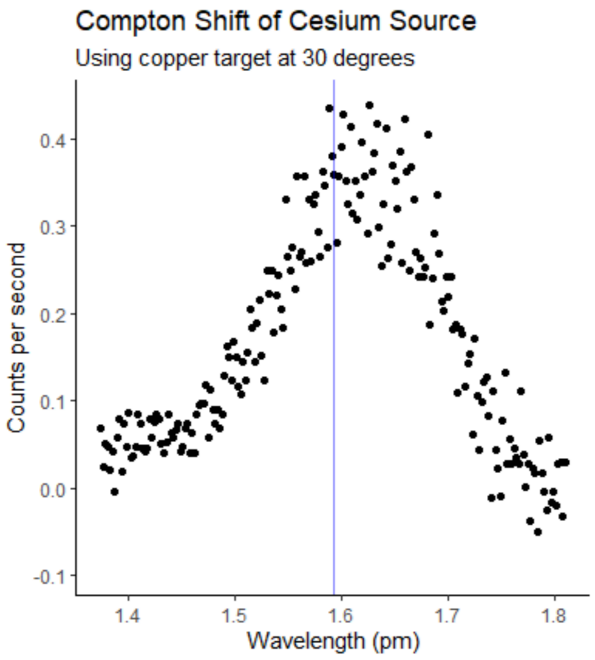

FIG. 3: A graph of the Compton shifted wavelength for cesium using a copper scattering target at 30 degrees. The ideal Compton shifted wavelength is indicated by the blue line.

We took the spectrum of the cesium source with the copper target at each angle and divided by time to normalize it to counts per second. We then took the background spectrum with no source and the background spectrum with the cesium source at each angle with no scattering target, and divided by time to normalize those. Subtracting out the background spectra from the spectra with the cesium source and copper target at each angle gave a final visualization of the Compton shift at each angle. At 10 degrees, the background spectra of cesium was at higher values than the scattered spectra, because the angle was too shallow. Results for this angle for cesium were therefore not useful and are not shown. An example of the Compton shift for cesium at 30° is given in Figure 3. The Compton shifts for all other angles are listed in the Appendix.

To obtain the Klein-Nishina relation for each source/target combination, we fit a normal distribution with Equation 4

$$f(x) = a\frac{1}{\sigma\sqrt{2\pi}}e^{-\frac{1}{2}(\frac{x-\mu}{\sigma})^2} \tag{4}$$

to the Compton-shifted peak at each angle, where a is the scale factor, μ is the mean of the distribution, and σ

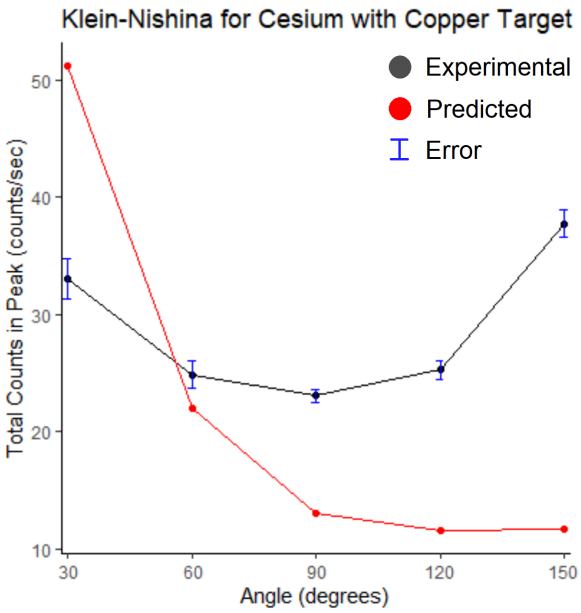

FIG. 4: The experimental Klein-Nishina relationship for the cesium source with a copper scattering target. It is compared with the idealized Klein-Nishina relation in red, as derived from Equation 2. A scale factor of 1/1,000 is applied to the predicted curve to fit on the scale of the experimental curve.

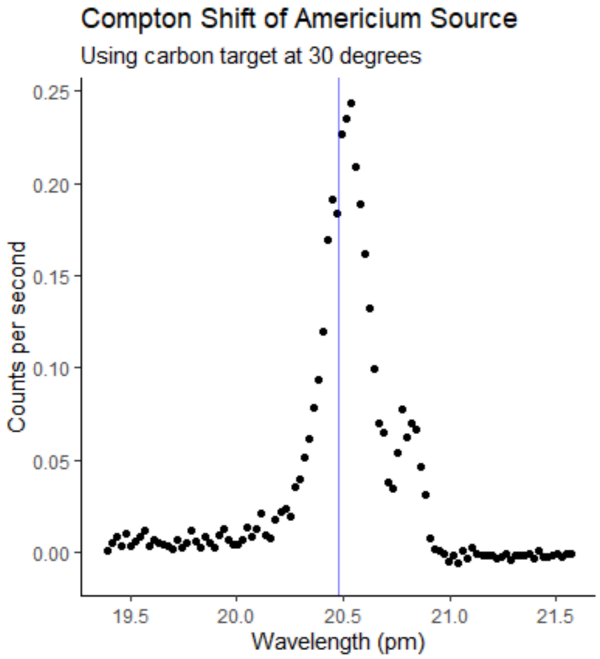

FIG. 5: A graph of the Compton shifted wavelength for americium using a carbon scattering target at 30 degrees. The ideal Compton shifted wavelength is indicated by the blue line.

is the standard deviation of the distribution. The mean μ provided the experimental Compton shift wavelength for each peak. a provided the area under the normal curve, since the area under a normal curve is 1 times its scale factor. This normal curve was made using the dnorm() function in R, which also provided error bars for a. The area under the curve represents the total count per second of Compton-shifted 661.7 kev gamma rays, which is proportional to the scattering cross-section of the photon as found in the Klein-Nishina Equation (2), because the scattering cross-section represents the probability of the gamma ray interacting with an electron in the detector. Given a long enough timescale, gamma rays are counted proportionally to their interaction probability. The Klein-Nishina graph for the cesium source with a copper scattering target is shown in Figure 4. The predicted Klein-Nishina function is scaled to fit on the same graph.

B. Low Energy Compton shifts

We conducted a similar process for the americium source using the Germanium detector instead. Am-241 releases gamma rays of 59.6keV, but also emits smaller amounts of gamma rays at 33 and 26 keV. Americium also decays into Plutonium and produces several X-rays, at 24.6 keV and lower [5].

We distinguish between the gamma rays and X-rays, and which gamma ray we want, during calibration by using the ratios between them and comparing them to the ratios between the peaks on the software to see which peak was which. We found the energies of these gamma and X-rays using the CRC Handbook of Chemistry and Physics [5].

For the americium source, we used a carbon cylinder target (3" tall cylinder with a 1/2" diameter) and a rectangular aluminum plate (1" x 3").

The proper wavelength for the Am-241 gamma ray of 59.6 keV is 20.8 pm. Figure 5 shows an example of the Compton shifted wavelength with americium off the carbon target at 30°. The same process was used to find the americium Compton shifts as cesium.

The Klein-Nishina graphs for each of the targets (carbon and aluminum) are shown in Figures 6 and 7. The same process was used to find the americium Klein-Nishina relation as cesium.

IV. CONCLUSIONS

The tables in Section **??** list the experimental and predicted Compton shift wavelengths of each source, target, and angle. These tables correspond to the graphs in Figures 8 9, and 10.

Changing the material of the scattering target did not affect the Compton shift wavelength, as expected according to Equation 1, but material did affect the width of the peak of the spectrum. For the americium source,

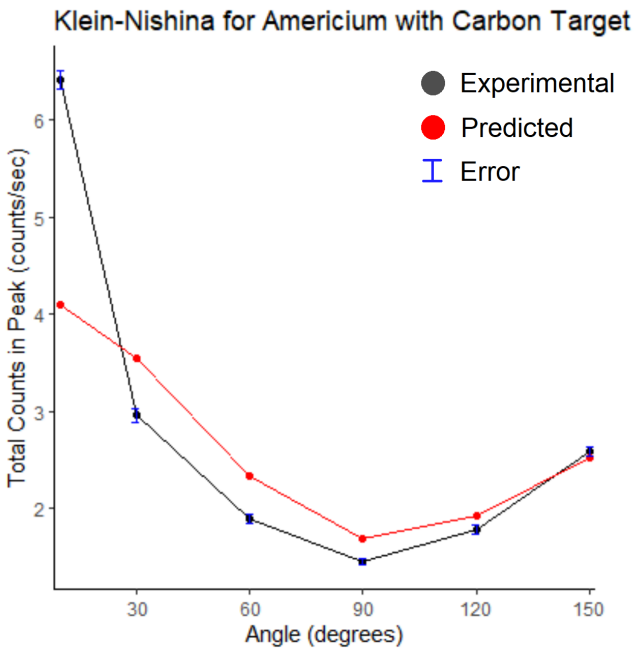

FIG. 6: The Klein-Nishina relation for the americium source with a carbon scattering target. It is compared with the idealized Klein-Nishina relation in red, as derived from Equation 2. A scale factor of 1/19,000 is applied to the predicted curve to fit on the scale of the experimental curve.

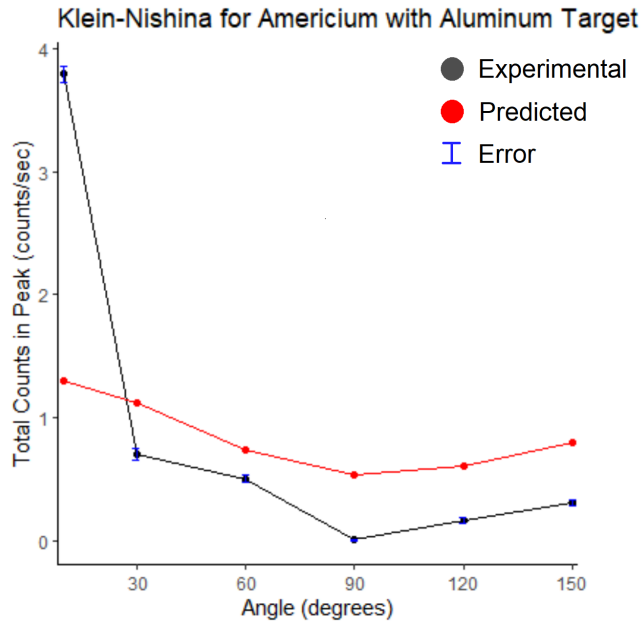

FIG. 7: The Klein-Nishina relation for the americium source with the aluminum scattering target. It is compared with the idealized Klein-Nishina relation in red, as derived from Equation 2. A scale factor of 1/60,000 is applied to the predicted curve to fit on the scale of the experimental curve.

the carbon target had much narrower peaks than aluminum. The width of the Compton shift peak is determined by the electron energy of the material. When a gamma ray impacts an atom, it scatters with a lowered energy according to Equation 1. However, if the electrons are in motion, there is a Doppler effect related to the projected velocities of the electrons. If the gamma ray imparts energy to the electron, the gamma ray's wavelength will increase, and if it gains energy from the electron, its wavelength will decrease. This causes Compton shifted gamma rays to increase or decrease in wavelength slightly, an effect known as Doppler broadening [6].

Overall, the experiment with americium was more accurate than that with cesium. All of the experimental Compton shifts for americium were 1% off of the value predicted by Equation 1, whereas the experimental Compton shifts for cesium were consistently 6-7% higher than the predicted value. This difference is likely due to inefficient background noise subtraction. While we simply subtracted the counts per second of the background spectrum from the scattered spectrum at each wavelength, it would have been more accurate to create a smoothed function to describe the background before subtracting it. This practice reduces the Poisson noise of the background and therefore that of the resulting spectrum. The Compton-shifted peak for cesium spans a wider domain of wavelengths than the for americium, which further exacerbates this issue because the increased noise makes the location of the peak more unclear, and therefore increases our error.

The Klein-Nishina function described our results more accurately for americium than cesium as well. For americium, the result of Equation 2, multiplied by a proportionality constant, describes the experimentally found curve accurately except for at 10 degrees, where the experimental result was much higher than expected. For cesium. The result of Equation 2 did not describe the experimental results well. The experimentally found curve for cesium decreases until a minimum at 90 degrees and then increases again, similar to that of americium. However, the Klein-Nishina function using the wavelength of 661.7 kev for the gamma rays of cesium decreases until a minimum at 180 degrees.

V. ACKNOWLEDGMENTS

Abstract: Em
Introduction: Sahar
Setup/Apparatus: Sahar
Experiment: Sahar
Conclusions: Em
Coding Graphs and Error bars: Em
Receiving (non)lethal doses of gamma rays: Sahar and Em
Forgetting to put the source in and collecting data for a solid 2 hours before noticing: Em and Sahar
The 4 PhD.'s putting up with way too much non-

sense (thanks): Joe Peidle, Matteo Mitrano, Jenny Hoffman, Jieping Fang

---

[1] A. H. Compton, A quantum theory of the scattering of x-rays by light elements, Physical Review **21**, 10.1103/PhysRev.21.483 (1923).

[2] The Compton Effect (2021), [Online; accessed 2021-11-11].

[3] Y. YAZAKI, How the klein–nishina formula was derived: Based on the sangokan nishina source materials, Proceedings of the Japan Academy, Series B **93**, 10.2183/pjab.93.025 (2017).

[4] A. A. Bartlett, Compton effect: Historical background, American Journal of Physics **32**, 10.1119/1.1970139 (1964).

[5] D. R. Lide, *CRC Handbook of Chemistry and Physics: : A ready-reference book of chemical and physical data.*, 77th ed. (1996).

[6] D. V. Rao, R. Cesareo, A. Brunetti, G. E. Gigante, T. Akatsuka, T. Takeda, and Y. Itai, Doppler broadening calculations of compton scattering for molecules, plastics, tissues, and few biological materials in the x-ray region: An analysis in terms of compton broadening and geometrical energy broadening, Journal of Physical and Chemical Reference Data **33**, 10.1063/1.1614814 (2004).

VI. APPENDIX

Compton Shift Results for Cesium and Copper Target			
Scattering Angle	Exper. Compton Shift Wavelength (pm)	Pred. Compton Shift Wavelength (pm)	Compton Shift Error
10^o	n/a	1.83	n/a
30^o	1.61	1.59	1.25%
60^o	1.20	1.13	6.11%
90^o	0.88	0.81	7.75%
120^o	0.68	0.63	7.78%
150^o	0.58	0.55	6.10%

TABLE I: The Compton shifted wavelengths of the cesium source and copper scattering target, compared with the predicted Compton shift (as calculated with equation 1). The error between the predicted and the measured shifted wavelength is also given. At 10 degrees, the background spectra of cesium was at higher values than the scattered spectra, because the angle was too shallow. Results for this angle for cesium were therefore not useful and are not shown.

Compton Shift Results for Cesium and Copper Target			
Scattering Angle	Exper. Compton Shift Wavelength (pm)	Pred. Compton Shift Wavelength (pm)	Compton Shift Error
10^o	n/a	1.83	n/a
30^o	1.61	1.59	1.25%
60^o	1.20	1.13	6.11%
90^o	0.88	0.81	7.75%
120^o	0.68	0.63	7.78%
150^o	0.58	0.55	6.10%

TABLE II: The Compton shifted wavelengths of the cesium source and copper scattering target, compared with the predicted Compton shift (as calculated with equation 1). The error between the predicted and the measured shifted wavelength is also given. At 10 degrees, the background spectra of cesium was at higher values than the scattered spectra, because the angle was too shallow. Results for this angle for cesium were therefore not useful and are not shown.

Compton Shift Results for Americium and Aluminum Target			
Scattering Angle	Exper. Compton Shift Wavelength (pm)	Pred. Compton Shift Wavelength (pm)	Compton Shift Error
10^o	20.81	20.76	0.20%
30^o	20.59	20.48	0.53%
60^o	19.75	19.65	0.52%
90^o	18.57	18.62	0.29%
120^o	17.72	17.70	0.14%
150^o	17.08	17.08	0.00%

TABLE III: The Compton shifted wavelengths of the americium source and aluminum scattering target, compared with the predicted Compton shift (as calculated with equation 1). The error between the predicted and the measured shifted wavelength is also given.

Compton Shift Results for Americium and Carbon Target			
Scattering Angle	Exper. Compton Shift Wavelength (pm)	Pred. Compton Shift Wavelength (pm)	Compton Shift Error
10^o	20.80	20.76	0.20%
30^o	20.52	20.48	0.19%
60^o	19.70	19.65	0.22%
90^o	18.67	18.62	0.23%
120^o	17.78	17.70	0.46%
150^o	17.12	17.08	0.26%

TABLE IV: The Compton shifted wavelengths of the americium source and carbon scattering target, compared with the predicted Compton shift (as calculated with equation 1). The error between the predicted and the measured shifted wavelength is also given.

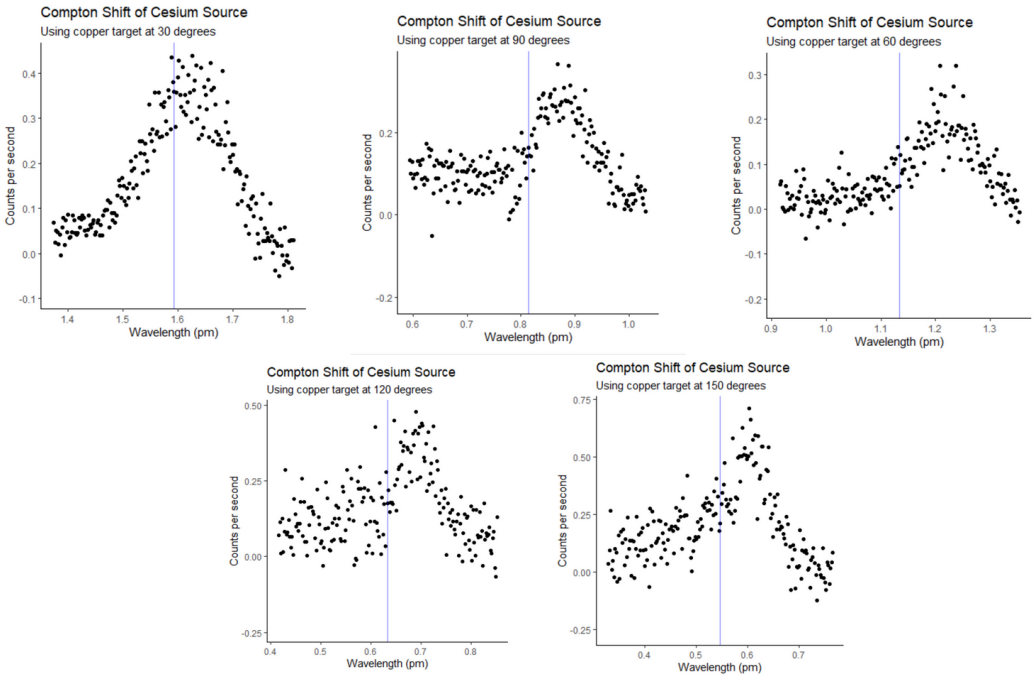

FIG. 8: The Compton shifts for cesium with the copper scattering target, at angles 30°,60°, 90°, 120°, and 150°.

FIG. 9: The Compton shifts for americium with the carbon scattering target, at angles 10°, 30°, 60°, 90°, 120°, and 150°.

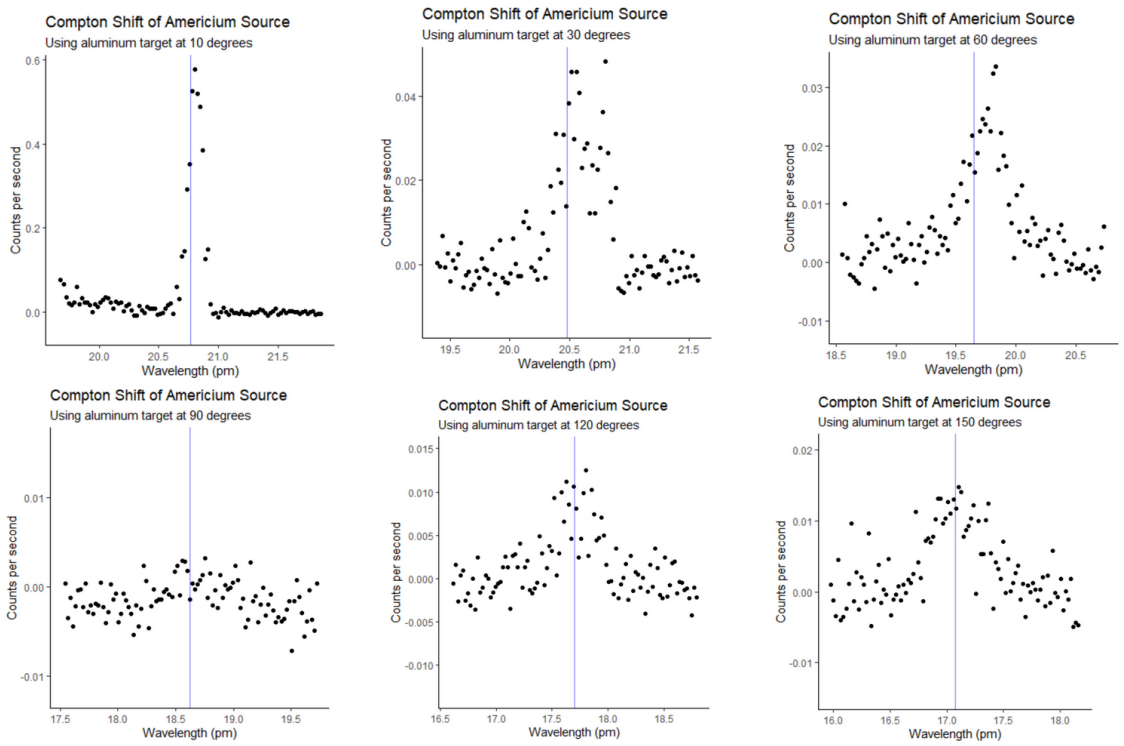

FIG. 10: The Compton shifts for americium with the aluminum scattering target, at angles 10°, 30°, 60°, 90°, 120°, and 150°.